

Finite temperature phase diagram of trapped Fermi gases with population imbalance

Wei Zhang and L.-M. Duan

FOCUS center and MCTP, Department of Physics, University of Michigan, Ann Arbor, MI 48109

(Dated: November 2, 2018)

We consider a trapped Fermi gas with population imbalance at finite temperatures and map out the detailed phase diagram across a wide Feshbach resonance. We take the Larkin-Ovchinnikov-Fulde-Ferrel (LOFF) state into consideration and minimize the thermodynamical potential to ensure stability. Under the local density approximation, we conclude that a stable LOFF state is present only on the BCS side of the Feshbach resonance, but not on the BEC side or at unitarity. Furthermore, even on the BCS side, a LOFF state is restricted at low temperatures and in a small region of the trap, which makes a direct observation of LOFF state a challenging task.

PACS numbers: 03.75.Ss, 03.75.Hh, 05.30.Fk

I. INTRODUCTION

There has been considerable interest in paired superfluidity of trapped Fermi gases, where the interatomic interaction can be tuned by varying the external magnetic field [1, 2, 3]. Recently, the experimental realization of superfluidity in polarized Fermi gases attracts great attention, where the numbers N_{\uparrow} and N_{\downarrow} of the two atomic species undergoing pairing are different [4, 5, 6]. This population imbalance is obviously detrimental to superfluidity, since the Cooper pairing requires equal number of atoms from both spin components. Therefore, by increasing the population imbalance from zero, it is expected that the BCS pairing state becomes less favorable and eventually gives its way to the normal or other exotic phases [7, 8, 9, 10, 11, 12].

One of the most fascinating phenomena in unbalanced Fermi systems is the Larkin-Ovchinnikov-Fulde-Ferrel (LOFF) states, which was first discussed as a "compromise" candidate exhibiting both pairing and non-zero magnetization in the context of superconductors in the presence of a magnetic field [7]. This exotic LOFF state is characterized by an order parameter with one or more non-zero components at finite momenta \mathbf{q} , hence breaks translational and rotational symmetry and forms a crystal of pairing order (i.e., a supersolid). In the past several decades, the existence of LOFF states was studied in various systems [13], including heavy fermions [14] and dense quark matter [15].

Comparing to the systems mentioned above, ultra-cold Fermi gases provide a super clean experimental platform with remarkable controllability, so that they can be studied with nearly arbitrary interaction strength and population imbalance. Therefore, after the realization of paired superfluidity in resonantly interacting ${}^6\text{Li}$ atoms with population imbalance [4, 5], the interest of LOFF state in these systems has been greatly intensified. Up to now, no evidence of LOFF state has been found yet in experiments on the polarized Fermi gas. Theoretically, some existing studies give significantly different predictions on the stable region of LOFF state: some works on the homogeneous system conclude that at zero temperature the LOFF state is confined to a narrow parameter

region on the BCS side of the resonance, for both cases of a narrow [16] and a wide [17] Feshbach resonance; while some other calculations claim a much larger region of a stable LOFF state [18, 19, 20], well existing at the unitarity point. What is subtle for these calculations is to implement a right set of stability conditions, which are usually controversial. Considering that there exist various possible competing phase configurations for this system, one thus needs to carefully distinguish a stable phase from some metastable states or unstable saddle point solutions.

In this manuscript, we consider the possibility of LOFF state and map out the detailed finite temperature phase diagram for fermionic atoms in a trap with population imbalance. To ensure stability, we directly minimize the thermodynamical potential instead of using the order parameter equations, as the latter may give unstable or metastable solutions [21]. The calculation of the full landscape of thermodynamical potential sounds to us the only method capable to distinguish a local metastable configuration from a globally stable phase. To deal with the trap, we use the local density approximation (LDA) which is typically valid unless the trap has a strong anisotropy and/or the total atom number is small [5, 22, 23]. Our main results are as follows. (i) We conclude that a stable LOFF state can only be present on the BCS side of the Feshbach resonance. On the BEC side and at the unitarity, the LOFF state is only a metastable state. (ii) Even on the BCS side of the resonance, a globally stable LOFF state is only restricted at low temperatures and in a small region of the trap. In a wider temperature and spatial region, the LOFF state is only a metastable state. Considering experimental limit of temperature and resolution, we expect that a direct observation of stable LOFF states is challenging for polarized Fermi gases in typical harmonic traps.

The remainder of this manuscript is organized as follows. In Section II, we discuss our formalism for unbalanced Fermi gases in an isotropic harmonic trap. We first derive a Ginzburg-Landau theory for the second order normal-LOFF and normal-BCS phase transitions, and then derive the mean-field thermodynamical potential to study the first order normal-LOFF and LOFF-

BCS phase transitions. In the mean-field calculation, for simplicity, we focus on the single-plane-wave LOFF state (i.e., the FF state). Our main results are presented in Section III, where the phase diagrams showing various stable or metastable states are illustrated for systems at unitarity, and on the BCS and BEC sides of the Feshbach resonance.

II. THE FORMALISM FOR POLARIZED FERMI GASES IN A HARMONIC TRAP

Since the population of closed channel molecules is negligible close to a wide Feshbach resonance [24, 25], we study a trapped Fermi gas by considering the following single-channel Hamiltonian (we use the natural unit such that $\hbar = k_B = 1$ throughout this manuscript):

$$\begin{aligned} \mathcal{H} = & \sum_{\mathbf{k}, \sigma} \xi_{\mathbf{k}, \sigma} a_{\mathbf{k}, \sigma}^\dagger a_{\mathbf{k}, \sigma} \\ & + \sum_{\mathbf{k}, \mathbf{k}', \mathbf{q}} V(\mathbf{k}, \mathbf{k}') a_{\mathbf{q}/2+\mathbf{k}, \uparrow}^\dagger a_{\mathbf{q}/2-\mathbf{k}, \downarrow}^\dagger a_{\mathbf{q}/2-\mathbf{k}', \downarrow} a_{\mathbf{q}/2+\mathbf{k}', \uparrow}, \end{aligned} \quad (1)$$

where $a_{\mathbf{k}, \sigma}^\dagger$ and $a_{\mathbf{k}, \sigma}$ are creation and annihilation operators for fermions labeled by the spin (hyperfine state) indices $\sigma = \uparrow, \downarrow$, respectively, and $\xi_{\mathbf{k}, \sigma} = \epsilon_{\mathbf{k}} - \mu_\sigma$ is the fermion dispersion $\epsilon_{\mathbf{k}} = k^2/(2m)$ shifted by the corresponding chemical potential. The attractive fermion-fermion interaction $V(\mathbf{k}, \mathbf{k}')$ can be written in a BCS form as $V(\mathbf{k}, \mathbf{k}') = -g$, provided that only s -wave contact interaction is considered. The interaction strength g can be connected with scattering parameters through the standard renormalization relation

$$-\frac{1}{g} = \frac{\mathcal{N}_0}{k_F a_s} - \sum_{\mathbf{k}} \frac{1}{2\epsilon_{\mathbf{k}}}, \quad (2)$$

where $\mathcal{N}_0 = mL^3 k_F / (4\pi)$ with Fermi momentum k_F and quantization volume L^3 , and a_s is the s -wave scattering length. In the following discussion, we take the local density approximation such that $\mu_\uparrow = \mu(\mathbf{r}) + h$, $\mu_\downarrow = \mu(\mathbf{r}) - h$, and $\mu(\mathbf{r}) = \mu_0 - U(\mathbf{r})$, where $U(\mathbf{r}) = m\omega^2 r^2/2$ represents an external harmonic trap [26]. The chemical potential at the trap center μ_0 and the chemical potential imbalance h can be related to the total particle number $N = N_\uparrow + N_\downarrow$ and the population imbalance $P = (N_\uparrow - N_\downarrow)/(N_\uparrow + N_\downarrow)$.

Using the functional integral technique, we introduce the standard Hubbard-Stratonovich field Δ which couples to $a^\dagger a^\dagger$ in order to integrate out the fermions, leading to the partition function

$$\mathcal{Z} = \text{Tr} (e^{-\beta \mathcal{H}}) = \int \mathcal{D}[\Delta^\dagger, \Delta] \exp \{-S_{\text{eff}}[\Delta^\dagger, \Delta]\} \quad (3)$$

with the effective action

$$S_{\text{eff}}[\Delta^\dagger, \Delta] = \int_0^\beta \frac{d\tau}{\beta} \sum_{\mathbf{k}} \left\{ \frac{\beta |\Delta|^2}{g} - \text{Tr} \ln (\beta \mathbf{G}^{-1}[\Delta]) \right\}, \quad (4)$$

where $\Delta \equiv \Delta(\mathbf{q}, \tau)$ depends on momentum \mathbf{q} and imaginary time τ , $\beta = 1/T$ is the inverse temperature, and \mathbf{G}^{-1} is the inverse fermion propagator

$$\mathbf{G}^{-1}[\Delta(\mathbf{q}, \tau)] = \begin{pmatrix} -\partial_\tau + \xi_\uparrow & \Delta(\mathbf{q}, \tau) \\ \Delta^\dagger(\mathbf{q}, \tau) & -\partial_\tau - \xi_\downarrow \end{pmatrix}. \quad (5)$$

Up to now we have not incorporated any approximation and the effective action Eq. (4) is accurate. Next, we will discuss in the rest of this section two approximation schemes, which can be applied to various situations. In section II A, a Ginzburg-Landau (GL) theory is presented to study the second order normal-LOFF and normal-BCS phase transitions. In section II B, a mean-field approach is applied to derive thermodynamical potential, such that the possibilities of first order normal-BCS and LOFF-BCS phase transitions can be analyzed.

A. Ginzburg-Landau theory and 2nd order phase transitions

In this section, we consider only the possibility of second order phase transitions from normal to superfluid phase, including both ordinary BCS and exotic LOFF states. Close to the phase transition line, the order parameter $\Delta(\mathbf{q}, \tau)$ has small magnitude, hence the effective action S_{eff} can be expanded in powers of Δ . In the spirit of Ginzburg-Landau (GL) theory, we are interested in static $\Delta(\mathbf{q})$. Therefore, the effective action takes the form

$$S_{\text{eff}} \approx \sum_{\mathbf{q}} \alpha(\mathbf{q}) |\Delta(\mathbf{q})|^2 + \mathcal{O}(\Delta^4), \quad (6)$$

where $\alpha(\mathbf{q}) = g^{-1} - \chi(\mathbf{q}, 0)$ with $\chi(\mathbf{q}, 0)$ is the pair susceptibility. Notice that as $\alpha(\mathbf{q})$ depends only on the magnitude of wave vector \mathbf{q} , the fourth order terms are crucial to determine the crystalline structures of the LOFF state [13]. However, when we getting very close to the phase transition line where the effective action is dominated by the leading quadratic term, it is sufficient to consider the coefficient $\alpha(\mathbf{q})$, leading to

$$\begin{aligned} \alpha(\mathbf{q}) = & \sum_{\mathbf{k}} \left[\frac{1}{2\epsilon_{\mathbf{k}}} - \frac{1 - n_F(\xi_{\mathbf{k}\mathbf{q},+}) - n_F(\xi_{\mathbf{k}\mathbf{q},-})}{2\xi_{\mathbf{k}\mathbf{q}}} \right] \\ & - \frac{\mathcal{N}_0}{k_F a_s}, \end{aligned} \quad (7)$$

where $n_F(x) \equiv (e^{\beta x} + 1)^{-1}$ is the Fermi distribution, $\xi_{\mathbf{k}\mathbf{q}, \pm} = \xi_{\mathbf{k}\mathbf{q}} \pm (\delta\epsilon_{\mathbf{k}\mathbf{q}} - h)$, $\xi_{\mathbf{k}\mathbf{q}} = \sum_{\sigma} (\xi_{\mathbf{k}+\mathbf{q}, \sigma} + \xi_{\mathbf{k}, \sigma})/4$, and $\delta\epsilon_{\mathbf{k}\mathbf{q}} = (\epsilon_{\mathbf{k}+\mathbf{q}} - \epsilon_{\mathbf{k}})/2$. As concluded in the GL theory, the normal state with $\Delta(\mathbf{q}) = 0$ loses its stability as long as $\alpha(\mathbf{q})$ becomes negative for one or more \mathbf{q} components. Therefore, we introduce the order parameter equation, which corresponds to the condition that $\alpha(\mathbf{q})$ crosses zero

$$\frac{\mathcal{N}_0}{k_F a_s} = \sum_{\mathbf{k}} \left[\frac{1}{2\epsilon_{\mathbf{k}}} - \frac{1 - n_F(\xi_{\mathbf{k}\mathbf{q},+}) - n_F(\xi_{\mathbf{k}\mathbf{q},-})}{2\xi_{\mathbf{k}\mathbf{q}}} \right]. \quad (8)$$

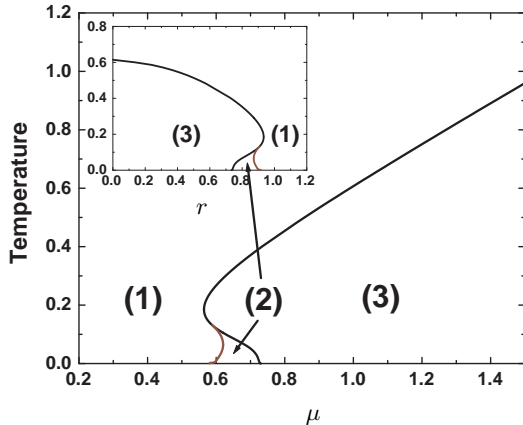


FIG. 1: Temperature versus chemical potential phase diagram is illustrated by solving Eq. (8) at unitarity, showing three different regions: (1) normal state is stable or metastable, (2) normal state loses its stability at $\mathbf{q} \neq 0$, and (3) normal state loses its stability at $\mathbf{q} = 0$. In this figure, the chemical potential difference $h = 0.4$ with arbitrary energy unit. Inset: The T - r diagram can be obtained by incorporating the LDA approximation. Here, we choose the energy unit as the chemical potential at the trap center $\mu_0 = 1$, and $h = 0.4$ in this scale. The radius r is in unit of $r_0 \equiv \sqrt{2\mu_0/(m\omega^2)}$.

This order parameter equation can be solved for a given $\mu(\mathbf{r})$ and h to obtain the normal-BCS transition temperature $T_c(\mathbf{q} = 0)$, while the normal-LOFF transition temperature is determined by the maximal $T_c(\mathbf{q})$ for all finite $\mathbf{q} \neq 0$. In Fig. 1, a typical T - μ phase diagram is depicted showing three different regions, where: (1) normal state is stable or metastable [$\alpha(\mathbf{q}) > 0$ for all \mathbf{q}], (2) normal state is unstable due to LOFF instabilities [$\alpha(0) > 0$, but $\alpha(\mathbf{q}) < 0$ for some finite \mathbf{q} 's], and (3) normal state is unstable due to BCS instability [$\alpha(0) < 0$]. Notice that at unitarity, the scattering parameter $a_s \rightarrow \infty$ and does not set up a length or energy scale. Therefore, phase diagrams for different values of h (as long as $h \neq 0$) are identical when an appropriate energy unit is applied. Furthermore, by incorporating the local density approximation (LDA) $\mu(\mathbf{r}) = \mu_0 - U(\mathbf{r})$, this T - μ phase diagram can be easily transformed into the T - r plane (r is the radius of the trap, see inset of Fig. 1), which can be related to experiments.

It should be emphasized that the phase diagrams obtained by solving the GL equation (8) is not a result within mean-field [16] or NSR schemes [27, 28], since the according approximated number equations are not included for self-consistent solving. Therefore, under the assumption that the order parameter is small, the GL theory discussed above is well controlled and the results are reliable. However, the small order parameter restric-

tion sets a limit of this approach only for analyzing second order phase transitions. The complete phase diagram, where the possibilities of first order phase transitions have to be taken into consideration, is beyond the scope of GL theory since $|\Delta|$ is not necessarily small. Thus, we discuss in the next subsection a mean-field approach to derive the thermodynamical potential, which offers an approximation technique to study the complete phase diagram by direct minimization.

B. Mean-field theory and 1st order phase transitions

Unlike the GL expansion of effective action Eq. (4) discussed above, a mean-field theory is considered here by introducing a uniform static saddle point $\Delta(\mathbf{q}, \tau) = \Delta_{\mathbf{Q}}\delta(\mathbf{q} - \mathbf{Q})$, which corresponds to the BCS state for $\mathbf{Q} = 0$, and to the single-plane-wave LOFF state for finite \mathbf{Q} . With this assumption, the saddle point action is

$$S_0 = \beta \frac{|\Delta_{\mathbf{Q}}|^2}{g} + \sum_{\mathbf{k}} \left\{ \beta (\xi_{\mathbf{k}\mathbf{Q}} - E_{\mathbf{k}\mathbf{Q}}) + \ln [n_F(-E_{\mathbf{k}\mathbf{Q},+})] + \ln [n_F(-E_{\mathbf{k}\mathbf{Q},-})] \right\}, \quad (9)$$

where $E_{\mathbf{k}\mathbf{Q}} = \sqrt{\xi_{\mathbf{k}\mathbf{Q}}^2 + \Delta_{\mathbf{Q}}^2}$, and $E_{\mathbf{k}\mathbf{Q},\pm} = E_{\mathbf{k}\mathbf{Q}} \pm (\delta\epsilon_{\mathbf{k}\mathbf{Q}} - h)$ is the quasiparticle energy (+) or the negative of the quasihole energy (-).

The saddle point conditions $\delta S_0 / \delta \Delta_{\mathbf{Q}}^\dagger = 0$ and $\delta S_0 / \delta |\mathbf{Q}| = 0$ lead to the order parameter equations

$$\begin{aligned} \frac{\mathcal{N}_0}{k_F a_s} &= \sum_{\mathbf{k}} \left[\frac{1}{2\epsilon_{\mathbf{k}}} - \frac{1 - n_F(E_{\mathbf{k}\mathbf{Q},+}) - n_F(E_{\mathbf{k}\mathbf{Q},-})}{2E_{\mathbf{k}\mathbf{Q}}} \right], \\ 0 &= \sum_{\mathbf{k}} (|\mathbf{Q}| - k_z) \left\{ [1 + n_F(E_{\mathbf{k}\mathbf{Q},+}) - n_F(E_{\mathbf{k}\mathbf{Q},-})] \right. \\ &\quad \left. + \frac{\xi_{\mathbf{k}\mathbf{Q}}}{E_{\mathbf{k}\mathbf{Q}}} [-1 + n_F(E_{\mathbf{k}\mathbf{Q},+}) + n_F(E_{\mathbf{k}\mathbf{Q},-})] \right\}, \quad (10) \end{aligned}$$

which can be solved together to determine Δ and $|\mathbf{Q}|$. Here, $k_z = |\mathbf{k}| \cos \theta$ with θ is the polar angle. However, solving these two order parameter equations is not sufficient to determine the phase diagram, since the solutions may be metastable states or only unstable saddle points. Therefore, to ensure stability, we evaluate and directly minimize the thermodynamic potential $\Omega_0 = S_0/\beta$, instead of imposing various subtle stability criteria [16, 20].

We show in Fig 2 a typical contour plot of the thermodynamic potential Ω_0 as functions of Δ and $|\mathbf{Q}|$, where lighter regions denote lower Ω_0 . Notice that the normal phase occurs at $\Delta = 0$ for all values of $|\mathbf{Q}|$. In this plot, two local minima are present, corresponding to the normal ($\Delta = 0$) and the BCS ($\Delta \neq 0, |\mathbf{Q}| = 0$) states, respectively. Combining the results together with those

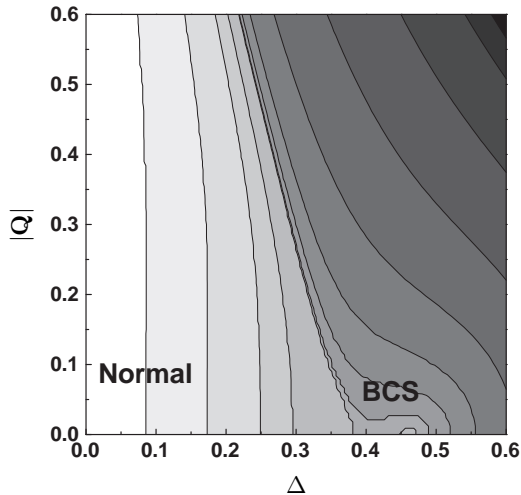


FIG. 2: Contour plots of mean-field thermodynamic potential Ω_0 as a function of Δ and wave vector $|\mathbf{Q}|$. Two local minima (lighter region) are shown to characterize the normal ($\Delta = 0$) and the BCS ($\Delta \neq 0, |\mathbf{Q}| = 0$) states. In this plot, parameters are chosen as $h = 0.4$, $\mu = 0.5$, $T = 0.1$, and $1/(k_F a_s) = 0$ (at unitarity), with arbitrary energy unit.

obtained from the GL theory, we can get more information about the finite temperature phase diagrams of trapped Fermi gases, which are discussed next.

III. FINITE TEMPERATURE PHASE DIAGRAM OF TRAPPED FERMI GASES WITH POPULATION IMBALANCE

Up to now, we discuss a GL theory which is valid for the small order parameter regime but not constrained by any approximation schemes, as well as a mean-field approach which is approximate but works for wider regions. Using these methods and the LDA approximation, we are able to analyze the finite temperature phase diagrams of polarized Fermi gases in harmonic traps. Next, we first consider in Section III A the case of unitarity, where the scattering length a_s does not set a length or energy scale, leading to the presence of universality. In Section III B, we discuss the weakly interacting BCS regime, where emphasis is put on the possibility of a stable LOFF state. Lastly, the strongly interacting BEC regime is studied in Section III C.

A. Unitarity

Following the formalism outlined in the previous section, we first map out the phase diagram for trapped

fermions at unitarity. The different phases in the trap can be identified from the global minimum of the mean-field thermodynamic potential at order parameter Δ and wave vector \mathbf{Q} . At zero temperature, there are three phases which could be possibly present: (i) a BCS superfluid state with $\Delta \neq 0$ at $|\mathbf{Q}| = 0$; (ii) a normal mixed state (NM) with $\Delta = 0$ and two Fermi surfaces ($\mu_\uparrow, \mu_\downarrow > 0$); and (iii) a normal polarized state (NP) with $\Delta = 0$ and one Fermi surface ($\mu_\uparrow > 0, \mu_\downarrow < 0$). The trap boundary is set when $\Delta = 0$ and both Fermi surfaces vanish ($\mu_\uparrow, \mu_\downarrow < 0$). However, at finite temperatures, both the trap boundary and the phase boundary between NM and NP are blurred.

We show in Fig. 3(a) the finite temperature phase diagram for a trapped Fermi gas with population imbalance. From the trap center to the edge, the BCS, normal mixed (NM), and normal polarized (NP) phases are identified sequentially. Furthermore, within the BCS phase, four regions can be identified due to the existence of normal and LOFF metastable states, which can be explicitly shown from the thermodynamic potential. At low temperatures, the thermodynamic potential acquire a double well structure near the trap edge. Starting from the trap edge, the normal minimum at $\Delta = 0$ is lower than the BCS minimum at ($\Delta \neq 0, |\mathbf{Q}| = 0$), while the relative order reverses after crossing the normal-BCS phase boundary [see Fig. 3(b)]. Continuing towards the trap center, the normal minimum becomes unstable due to LOFF instability, but remains stable for BCS instability. The LOFF instability can lead to a metastable LOFF state at low temperatures, as shown in Fig. 3(c). In this case, the global minimum in the landscape still corresponds to a BCS state. However, from the normal state to the BCS state, one needs to pass a potential barrier through a first-order phase transition. Further to the trap center or at higher temperature, the LOFF state loses its metastability such that the double well structure disappears and the BCS state becomes the only minimum in the landscape of the thermodynamic potential, as shown in Fig. 3(d). What is special in this case is that to go from a normal state to a BCS state (with $|\mathbf{Q}| = 0$), one needs to follow a path of LOFF instability with pair momentum $|\mathbf{Q}| \neq 0$ (there is no BCS instability at $|\mathbf{Q}| = 0$ when the order parameter Δ is small). As one moves even further towards the trap center, the normal minimum becomes unstable due to both LOFF and BCS instabilities, as illustrated in Fig. 3(e), and the system goes to the BCS phase directly through the BCS instability at $|\mathbf{Q}| = 0$, corresponding to a second order phase transition.

Considering the universality present at unitarity, the qualitative features of phase diagrams are identical for arbitrary values of $h > 0$, as shown in Fig. 4 (the temperature and phase boundaries get somewhat rescaled). Therefore, we can conclude that for a polarized Fermi gas in a harmonic trap where the interaction is tuned at resonance, a globally stable LOFF state can not be present on the finite temperature phase diagram, although there exist a small region of a metastable LOFF state and also

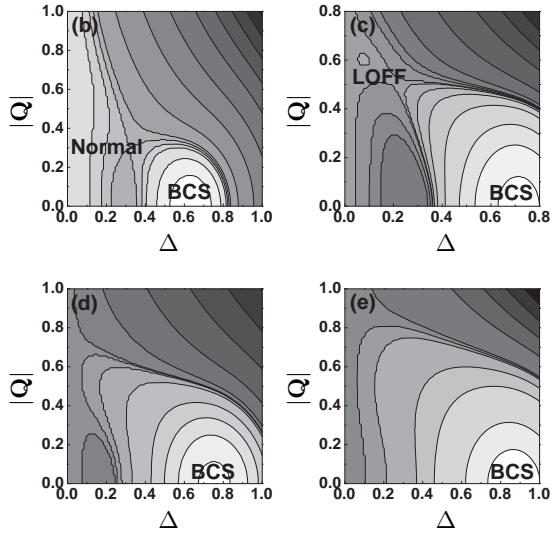
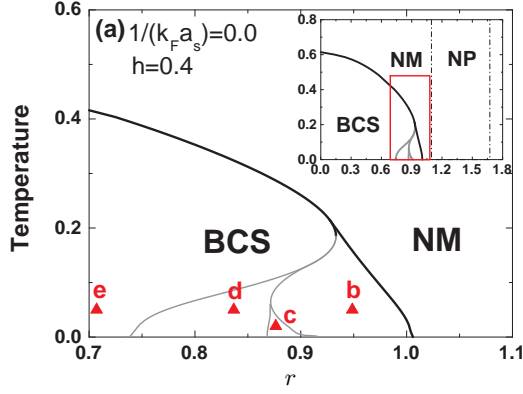


FIG. 3: (a) Finite temperature phase diagram of a polarized Fermi gas in a trap with $h = 0.4$ and $1/(k_F a_s) = 0$, where the chemical potential at the trap center μ_0 is used as energy unit, and $r_0 \equiv \sqrt{2\mu_0}/(m\omega^2)$ is used as length unit. The complete phase diagram is shown in the inset, while the selected area (rectangle) is zoomed in to show detailed structures. In this plot, a superfluid BCS, a normal mixed (NM), and a normal polarized (NP) states can be sequentially identified from trap center to trap edge. While the BCS and normal regions are separated by a phase transition line (dark solid), the trap boundary and the phase boundary between NM and NP (dot-dashed) are blurred at finite temperatures. Furthermore, within the BCS phase, four regions can be identified due to the existence of metastable normal and LOFF states (gray solid). The contours of thermodynamic potential at representative points of each region are plotted in (b-e), showing corresponding characteristic behaviors.

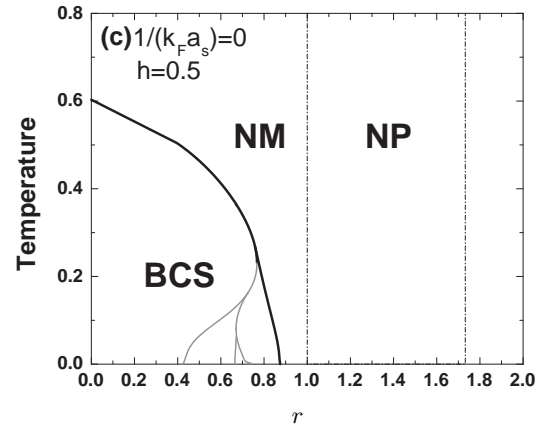
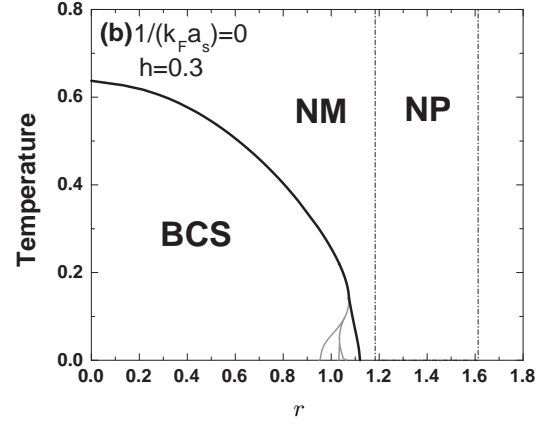
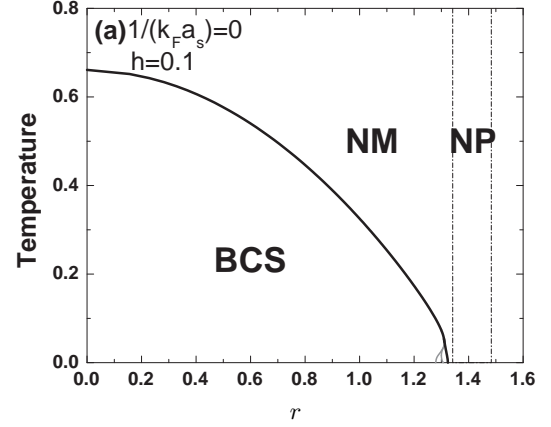


FIG. 4: Finite temperature phase diagrams of polarized Fermi gases in a harmonic trap at unitarity $1/(k_F a_s) = 0$, where the same energy and length units are used as in Fig. 3(a). Parameters used in these plots are (a) $h = 0.1$; (b) $h = 0.3$; and (c) $h = 0.5$.

a region where the normal state becomes unstable due to the LOFF instability (but still ends to a BCS state). This conclusion is consistent with the findings in Refs. [16] for the zero-temperature case, but does not agree with the outcomes in [18, 19, 20].

B. BCS regime

Comparing to the unitarity case, the phase diagrams on the BCS side of Feshbach resonances are more complicated. In Fig. 5(a), we show a typical case on the BCS regime. The most significant feature is the presence of a stable LOFF state at low temperatures, which is characterized by a global minimum of the thermodynamic potential at $\Delta(\mathbf{Q}) \neq 0$ with $|\mathbf{Q}| \neq 0$, as shown in the contour plots Fig. 5(f) and (g).

In addition to the presence of a stable LOFF state, the BCS phase also contains four regions which can be identified due to the existence of metastable normal and LOFF states. By evaluating the thermodynamic potential Ω_0 , the four regions can be characterized as Ω_0 : (i) has two minima corresponding to a stable BCS and a metastable normal states [see Fig. 5(b)]; (ii) has two minima corresponding to a stable BCS and a metastable LOFF states [see Fig. 5(c)]; (iii) has only one BCS minimum while the normal state is stable for BCS instability, but unstable for LOFF instability [see Fig. 5(d)]; and (iv) has only one BCS minimum and the normal state is unstable for BCS instability [see Fig. 5(e)].

It should be emphasized that unlike the unitarity case, universality is not present in the BCS regime, since the finite scattering parameter a_s sets an additional length or energy scale. Therefore, the characteristics of phase diagrams for various $1/(k_0 a_s) < 0$ and $h > 0$ are not identical. However, as shown in a series of phase diagrams in Fig. 6, we can summarize some common features within a qualitative level. First, the region where a LOFF state is stable is only present in the BCS regime, and disappears as one moves towards the unitarity [see Fig. 6(b)]. Second, a stable LOFF state is only present in a small region of the trap at low temperatures, and restricted for smaller chemical potential difference h . By increasing h (or equivalently polarization P), the region for stable LOFF state shrinks as shown in Fig. 6(c).

Although our calculation results can not be directly compared with experiments, where the total particle number and polarization are observables instead of μ_0 and h , the plots in Fig. 6 outline the general features of a finite temperature phase diagram in the BCS regime. Therefore, we can conclude that a stable LOFF state may be present in harmonically trapped Fermi gases with population imbalance, but only at low temperatures and in a small region of the trap.

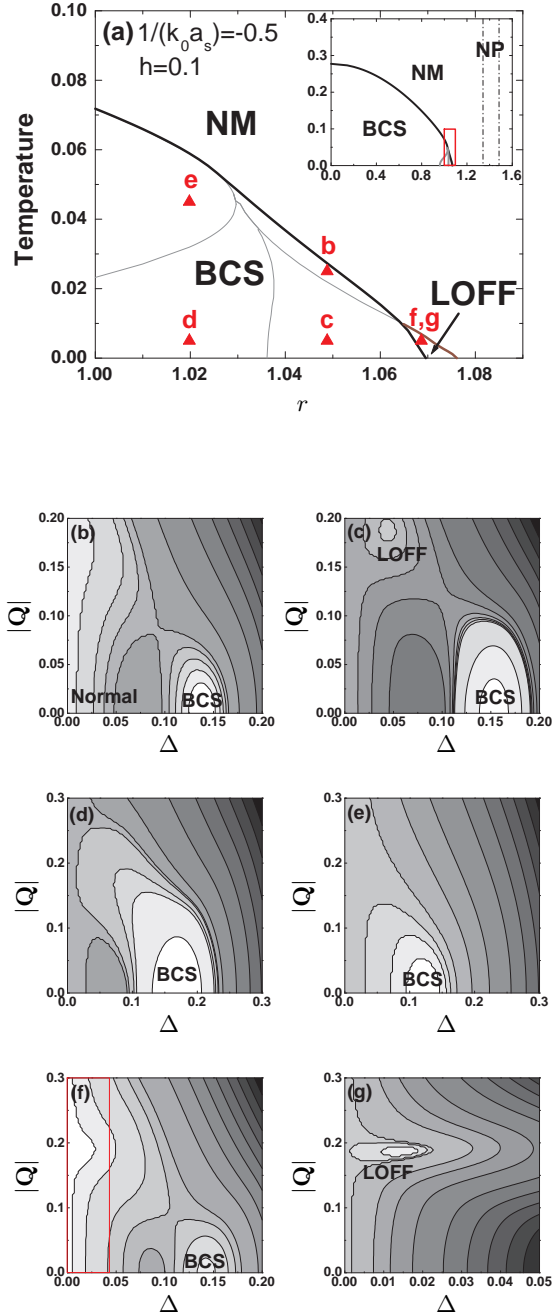


FIG. 5: (a) Finite temperature phase diagram for a polarized Fermi gas in a harmonic trap, showing the small region where a stable LOFF state is present. The complete phase diagram is shown in the inset, while the selected area (rectangle) is zoomed in to show the detailed structure. The parameters used in this plot are $h = 0.1$ and $1/(k_0 a_s) = -0.5$ (BCS regime), where $k_0 = \sqrt{2m\mu_0}$ with μ_0 is set as the energy unit. The radius r is in unit of $r_0 \equiv \sqrt{2\mu_0/(m\omega^2)}$. Within the BCS phase, four regions can be identified due to the stability of normal and LOFF states and how they are broken (gray solid). The thermodynamic potential at representative points of each region are plotted in (b-f), while (g) shows the detailed structure of the selected area (rectangle) in plot (f).

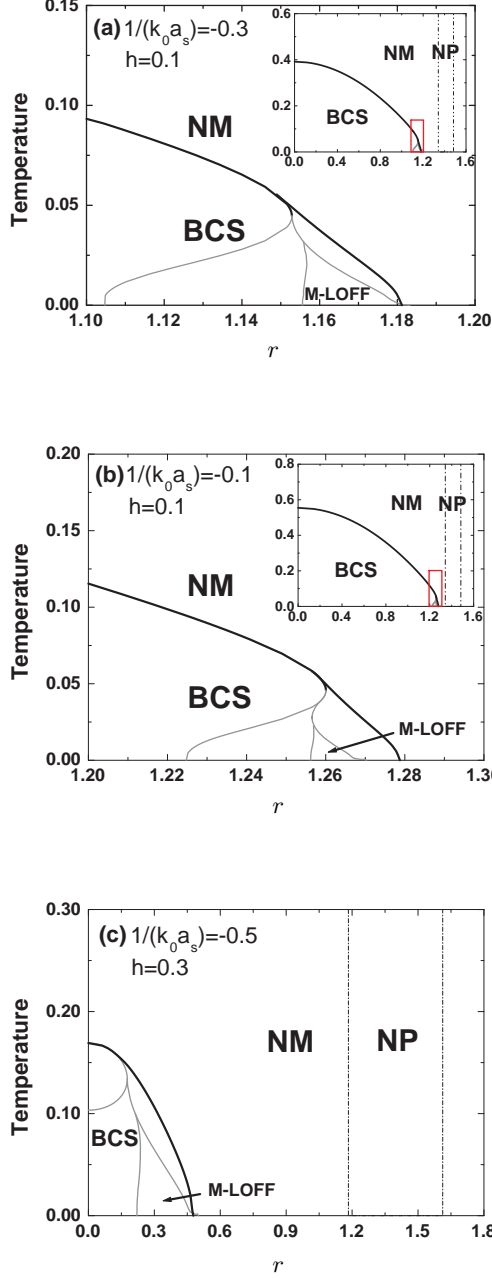


FIG. 6: Finite temperature phase diagrams of polarized Fermi gases in a harmonic trap in the BCS regime, with the same energy and length units as used in Fig. 5(a). In (a) and (b), the complete phase diagrams are shown in the insets, while the selected areas (rectangle) are zoomed in to show detailed structures. Notice in these two plots that for fixed chemical potential difference $h = 0.1$, the region with stable LOFF state becomes negligible and the region with metastable LOFF state [M-LOFF, also characterized by point c in Fig. 5(a)] shrinks as moving towards unity. Furthermore, if fixing the value of $1/(k_0 a_s) = -0.5$ as in Fig. 5, the stable LOFF state also almost disappears by increasing h to $h = 0.3$, as shown in (c). Other parameters used in these plots are (a) $1/(k_0 a_s) = -0.3$, and (b) $1/(k_0 a_s) = -0.1$, where $k_0 = \sqrt{2m\mu_0}$.

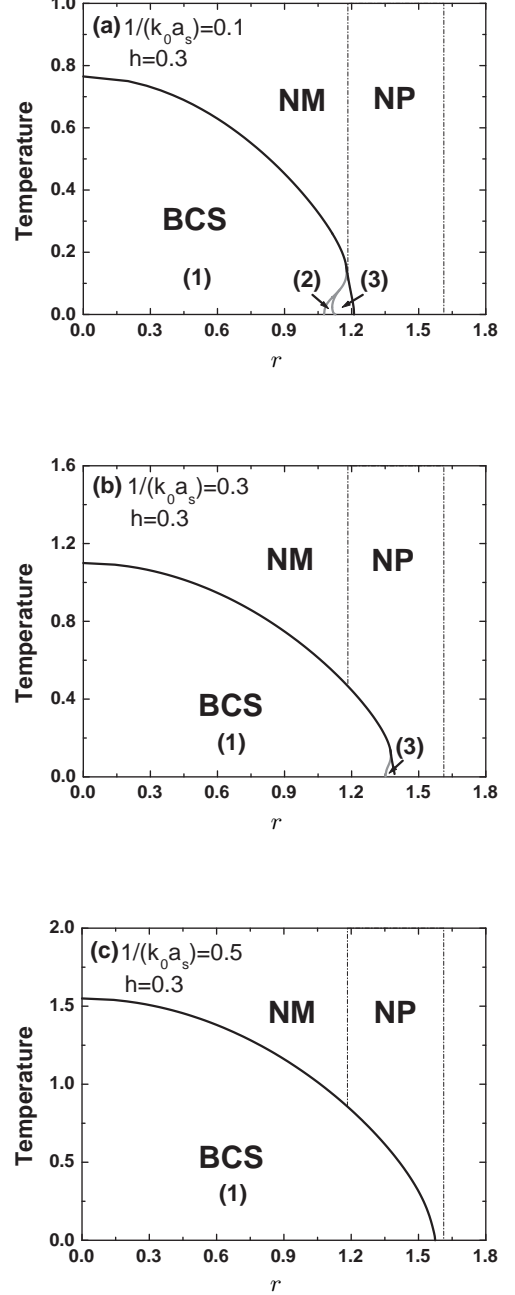


FIG. 7: Finite temperature phase diagrams of polarized Fermi gases in a harmonic trap in the BEC regime. The same energy and length units are used as in Fig. 6. Three regions may be present in these plots, where the thermodynamical potential (1) has only one BCS minimum and the normal state is unstable for BCS and LOFF instabilities; (2) has only one BCS minimum and the normal state is unstable only for LOFF instability; and (3) has two minima corresponding to a stable BCS and a metastable normal states. Parameters used in these plots are (a) $1/(k_0 a_s) = 0.1$, $h = 0.3$; (b) $1/(k_0 a_s) = 0.3$, $h = 0.3$; and (c) $1/(k_0 a_s) = 0.5$, $h = 0.3$, where $k_0 = \sqrt{2m\mu_0}$.

C. BEC regime

As concluded in the previous discussion, the LOFF state becomes less favorable as one moves from the BCS regime to the unitarity. As one further increases the interaction strength, the same trend is kept in the BEC regime, as shown in Fig. 7. Although the finite scattering length a_s sets an additional energy scale such that the phase diagrams are qualitatively different for various $1/(k_0 a_s) > 0$ and $h > 0$, there are still some general features which can be concluded. First, similar to the unitarity case, a stable LOFF state is not present on the finite temperature phase diagrams in the BEC regime. Second, the structure of the BCS phase becomes simpler and contains less sub-regions. By moving from the unitarity towards the BEC limit, the region with metastable LOFF state disappears first such that at the value of $1/(k_0 a_s) = 0.1$ [see Fig. 7(a)], only three regions are present in the BCS phase. By increasing the value of $1/(k_0 a_s)$, the region where the normal state becomes unstable only due to LOFF instability [region (2) in Fig. 7(a)] disappears, such that the BCS phase becomes even simpler as shown in Fig. 7(b). Further towards the BEC side, only a simple BCS superfluid state [region (1)] is present at the trap center, leading to a phase diagram similar to the unpolarized case [see Fig. 7(c)]. Notice that for the parameters used in these plots, the breached pair state (BP1) [10, 21] characterized by gapless fermionic excitations with a Fermi surface is not present at zero temperature. At finite temperatures, the boundary between BCS and BP1 is blurred and the crossover cannot be clearly distinguished.

IV. SUMMARY

We discuss in this manuscript the finite temperature phase diagrams of a trapped Fermi gas with population imbalance, focusing on the existence and stability of the LOFF state. We first derive a Ginzburg-Landau (GL) theory to study the second order normal-BCS and normal-LOFF phase transitions, where the order parameter is assumed to be small to ensure validity. Furthermore, in order to determine the complete phase diagram, we adopt the mean-field approximation and directly minimize the resulting thermodynamic potential. This method allows us to distinguish the stable, the metastable, and the unstable saddle point phases from solutions of the order parameter equations.

Using these methods, we are able to map out the finite-temperature phase diagrams over the BCS to BEC region. We show that a stable LOFF state exists only on the BCS side of the Feshbach resonance, but not at unitarity or in the BEC regime. Furthermore, we find that the LOFF state only exists at low temperatures within an appropriate region of population imbalance. With a global harmonic trap, even in the most optimal situation of all the parameters, the LOFF state is only present in a small region of the trap. With the experimental limits on temperature and spatial resolution, we expect that it is very challenging to make a direct observation of a stable LOFF state in typical harmonic traps.

This work is supported by the MURI, the DARPA, the NSF under grant number 0431476, the ARDA under ARO contracts, and the A. P. Sloan Foundation.

-
- [1] C. A. Regal, M. Greiner, and D. S. Jin, *Phys. Rev. Lett.* **92**, 040403 (2004).
 - [2] M. W. Zwierlein, C. A. Stan, C. H. Schunck, S. M. F. Raupach, A. J. Kerman, and W. Ketterle, *Phys. Rev. Lett.* **92**, 120403 (2004).
 - [3] C. Chin, M. Bartenstein, A. Altmeyer, S. Riedl, S. Jochim, J. Hecker Denschlag, and R. Grimm, *Science* **305**, 1128 (2004).
 - [4] M. W. Zwierlein, A. Schirotzek, C. H. Schunck, and W. Ketterle, *Science* **311**, 492 (2006).
 - [5] G. B. Partridge, W. Li, R. I. Kamar, Y. Liao, and R. G. Hulet, *Science* **311**, 503 (2006).
 - [6] M. W. Zwierlein, C. H. Schunck, A. Schirotzek, and W. Ketterle, *Nature* **442**, 54 (2006); Y. Shin, M. W. Zwierlein, C. H. Schunck, A. Schirotzek, and W. Ketterle, *Phys. Rev. Lett.* **97**, 030401 (2006); G. B. Partridge, W. Li, Y. A. Liao, R. G. Hulet, M. Haque, and H. T. Stoof, *Phys. Rev. Lett.* **97**, 190407 (2006).
 - [7] A. I. Larkin and Yu. N. Ovchinnikov, *Sov. Phys. JETP* **20**, 762 (1965); P. Fulde and R. A. Ferrel, *Phys. Rev.* **135**, A550 (1964).
 - [8] G. Sarma, *J. Phys. Chem. Solids* **24**, 1029 (1963).
 - [9] H. Muther and A. Sedrakian, *Phys. Rev. Lett.* **88**, 252503 (2002).
 - [10] W. V. Liu and F. Wilczek, *Phys. Rev. Lett.* **90**, 047002 (2003);
 - [11] P. F. Bedaque, H. Caldas, and G. Rupak, *Phys. Rev. Lett.* **91**, 247002 (2003).
 - [12] W. Yi and L.-M. Duan, *Phys. Rev. Lett.* **97**, 120401 (2006).
 - [13] R. Casalbuoni and G. Nardulli, *Rev. Mod. Phys.* **76**, 263 (2004).
 - [14] H. A. Radovan, N. A. Fortune, T. P. Murphy, S. T. Hannahs, E. C. Palm, S. W. Tozer, and D. Hall, *Nature* **425**, 51 (2003).
 - [15] M. Alford, J. A. Bowers, and K. Rajagopal, *Phys. Rev. D* **63**, 074016 (2001).
 - [16] D. E. Sheehy and L. Radzihovsky, *Phys. Rev. Lett.* **96**, 060401 (2006).
 - [17] W. Yi and L.-M. Duan, unpublished, see also the PhD thesis of W. Yi.
 - [18] K. Machida, T. Mizushima, and M. Ichioka, *Phys. Rev. Lett.* **97**, 120407 (2006).
 - [19] J. Kinnunen, L. M. Jensen, and P. Torma, *Phys. Rev. Lett.* **96**, 110403 (2006).
 - [20] Y. He, C.-C. Chien, Q. J. Chen, and K. Levin, *Phys. Rev. A* **75**, 021602(R) (2007).
 - [21] W. Yi and L.-M. Duan, *Phys. Rev. A* **73**, 031604(R) (2006).

- (2006); Phys. Rev. A **74**, 013610 (2006).
- [22] T. N. De Silva and E. J. Mueller, Phys. Rev. Lett. **97**, 070402 (2006).
- [23] For a strongly anisotropic trap where the system becomes almost one dimensional, the condition for the LOFF state may become less stringent, see, e.g., G. Orso, Phys. Rev. Lett. **98**, 070402 (2007); H. Hu, X.-J. Liu, and P. D. Drummond, Phys. Rev. Lett. **98**, 070403 (2007).
- [24] Q. J. Chen, J. Stajic, S. N. Tan, and K. Levin, Phys. Rep. **412**, 1 (2005).
- [25] W. Yi and L.-M. Duan, Phys. Rev. A **73**, 063607 (2006).
- [26] We assume here the trap has a spherical symmetry without loss of generality, as any non-spherical harmonic trap can be rescaled to a spherical one under the LDA [21].
- [27] M. M. Parish, F. M. Marchetti, A. Lamacraft, and B. D. Simons, Nature Phys. **3**, 124 (2007).
- [28] X.-J. Liu and H. Hu, Europhys. Lett. **74**, 574 (2006).